

$\bar{e} = -1.5\epsilon(k_F)[\epsilon(k_F) = 46.03 \text{ MeV}]$. Furthermore, we have put $z = 2\bar{e}$, i.e., an average value which is necessary for computing the single-particle energies below the Fermi level [see Eq. (8)]. Anyhow, the precise values of \bar{e} and z are not important at high momenta k_1 .

The results are shown in Fig. 4. Because of our approximations the curves are not reliable at momenta close to the Fermi momentum (compare Fig. 2).

Let us notice that V_{hbc} is comparatively close to V_{ho} for $k_1 \lesssim 6k_F$. For higher momenta k_1 , on the other hand, the kinetic energy $\hbar^2 k_1^2 / 2M$ becomes several times bigger than the potential energy V . Hence, one should not expect that we would get results very much different from those obtained in the present paper if we applied the hard-core potential instead of the "hollow-hard-core" potential.

All the computed single-particle potentials go to zero for extremely high momenta [V_{ho} goes through a

maximum at $k_1 \cong 13k_F$]. This is the result of considering the interaction in S , P , and D states only. If we included all partial waves we could perform the l sums in Eq. (A7) exactly, with the result⁴

$$V(k_1; k_1, z)_{\text{ho}}^{\text{IN}} \sim [k_1^2 - (M/\hbar^2)(z + \bar{e})]. \quad (\text{A9})$$

In the case of Eq. (A8), approximations similar to those which have led us to Eq. (A5) give⁴

$$V(k_1; k_1, z)_{\text{ho}}^{\text{S}} \sim \bar{a} \rightarrow (\sqrt{3/4})k_1. \quad (\text{A10})$$

[A comparison of the proportionality factor of Eq. (A10) with Eq. (A5) gives $V_{\text{hbc}} \cong 1.6V_{\text{ho}}^{\text{S}}$ at very high momenta.]

Hence, only for extremely high momenta ($k_1 \gtrsim 10k_F$) is $V_{\text{hbc}} \cong V_{\text{ho}}^{\text{IN}} \gg V_{\text{hbc}}$ when the interaction is included in all orbital states. However, as pointed out in Sec. VI, this range of momenta should not affect the properties of nuclear matter.

Excitation Functions for Nucleon and Alpha-Particle Transfer Reactions Induced by ^{14}N Ions*

R. M. GAEDKE,† K. S. TOH,‡ AND I. R. WILLIAMS
Oak Ridge National Laboratory, Oak Ridge, Tennessee
(Received 20 May 1965)

Nitrogen ions, accelerated in the ORNL 63-in. cyclotron and tandem Van de Graaff, were utilized in a study of nucleon and alpha-particle transfer reactions. The reaction products were identified by means of their characteristic gamma rays and half-lives, and quantitatively studied by radioactive assay. In all, 21 reactions were investigated. The following nucleon transfer reactions were studied: $^{12}\text{C}(^{14}\text{N}, ^{13}\text{N})^{13}\text{C}$; $^{16}\text{O}(^{14}\text{N}, ^{15}\text{N})^{17}\text{O}$; $^{16}\text{O}(^{14}\text{N}, ^{15}\text{N})^{18}\text{O}$; $^{19}\text{F}(^{14}\text{N}, ^{15}\text{N})^{18}\text{F}$; $^{31}\text{P}(^{14}\text{N}, ^{13}\text{N})^{32}\text{P}$; $^{45}\text{Sc}(^{14}\text{N}, ^{15}\text{N})^{44\text{m}}\text{Sc}$; $^{45}\text{Sc}(^{14}\text{N}, ^{15}\text{N})^{44\text{g}}\text{Sc}$; $^{51}\text{V}(^{14}\text{N}, ^{13}\text{N})^{52}\text{V}$; $^{55}\text{Mn}(^{14}\text{N}, ^{13}\text{N})^{56}\text{Mn}$; and $^{55}\text{Mn}(^{14}\text{N}, ^{15}\text{N})^{54}\text{Mn}$. For the ^{45}Sc target it was found that the isomer yield ratio, $^{44\text{m}}\text{Sc}/^{44\text{g}}\text{Sc}$, remained constant at a value of ~ 0.8 over the bombarding range 20–42 MeV. The ^{31}P reaction was investigated by the detection of both products. The yields obtained in these two ways were found to be equal, within experimental error, thus indicating that the ^{13}N (whose excited states are unstable with respect to particle emission) is left in its ground state. Three new values were determined for the ratio of the neutron reduced width in ^{14}N and ^{19}F by comparing $(^{14}\text{N}, ^{13}\text{N})$ reactions on ^{19}F , ^{51}V , and ^{55}Mn with $(^{19}\text{F}, ^{18}\text{F})$ data obtained by Perkin *et al.* on the same three target nuclei. Excitation functions were determined for $(^{14}\text{N}, ^{18}\text{F})$ reactions on the following targets: ^6Li , ^7Li , ^{12}C , ^{16}O , ^{19}F , and ^{27}Al . These data were examined together with previously available results for the same reaction on ^9Be and ^{10}B . It was noted that the cross sections at the Coulomb barrier energies show a strong dependence on the alpha-particle binding energy of the target nucleus; this suggests that at low incident energies the ^{18}F may be at least partially produced by the pickup of an alpha particle by the incident ^{14}N ion. Cross-section measurements were also made for the production of: ^{18}O from ^6Li and ^7Li ; ^{21}Na and ^{24}Na from ^{12}C ; ^{22}Na from ^{16}O ; and ^{38}K from ^{27}Al .

I. INTRODUCTION

A SURVEY of excitation functions for ^{14}N -induced reactions is presented in this paper. The cross-section measurements were begun at the ORNL 63-in. cyclotron, where the maximum nitrogen energy avail-

able was ~ 27.5 MeV. With the opportunity of obtaining 42-MeV ^{14}N ions at the ORNL tandem Van de Graaff, the measurements were then extended to the higher energy. At the tandem accelerator it was also possible, because of the added energy, to bombard some additional targets with higher atomic numbers.

The following nucleon transfer reactions were investigated: $^{12}\text{C}(^{14}\text{N}, ^{13}\text{N})^{13}\text{C}$; $^{16}\text{O}(^{14}\text{N}, ^{13}\text{N})^{17}\text{O}$; $^{16}\text{O}(^{14}\text{N}, ^{15}\text{N})^{17}\text{O}$; $^{16}\text{O}(^{14}\text{N}, ^{15}\text{N})^{18}\text{O}$; $^{19}\text{F}(^{14}\text{N}, ^{15}\text{N})^{18}\text{F}$; $^{31}\text{P}(^{14}\text{N}, ^{13}\text{N})^{32}\text{P}$; $^{45}\text{Sc}(^{14}\text{N}, ^{15}\text{N})^{44\text{m}}\text{Sc}$; $^{45}\text{Sc}(^{14}\text{N}, ^{15}\text{N})^{44\text{g}}\text{Sc}$; $^{51}\text{V}(^{14}\text{N}, ^{13}\text{N})^{52}\text{V}$; $^{55}\text{Mn}(^{14}\text{N}, ^{13}\text{N})^{56}\text{Mn}$; and $^{55}\text{Mn}(^{14}\text{N}, ^{15}\text{N})^{54}\text{Mn}$. The main purpose here

* Research sponsored by the U. S. Atomic Energy Commission under contract with the Union Carbide Corporation.

† Oak Ridge Graduate Fellow from the University of South Carolina, under appointment from the Oak Ridge Institute of Nuclear Studies.

‡ John Simon Guggenheim Fellow, 1965–66. Temporary address: Institute for Theoretical Physics, Copenhagen.

was to determine additional values for the ratio of the neutron reduced width in ^{14}N and ^{19}F . This is done by the comparison of pairs of reactions in which the same target nucleus has been bombarded with both ^{14}N and ^{19}F beams, leading to ($^{14}\text{N},^{13}\text{N}$) and ($^{19}\text{F},^{18}\text{F}$) neutron transfers, respectively.¹

Excitation functions were obtained for the production of ^{18}F by the nitrogen bombardment of ^6Li , ^7Li , ^{12}C , ^{16}O , and ^{27}Al . The purpose was to shed some light on the possibility that the ^{18}F could be produced by means of alpha-particle transfer from the target nuclei to the incoming ^{14}N ions. Cross-section measurements were also made for the production of: ^{15}O from ^6Li and ^7Li ; ^{21}Na and ^{24}Na from ^{12}C ; ^{22}Na from ^{16}O ; and ^{38}K from ^{27}Al .

II. EXPERIMENTAL METHOD

The following materials were used as targets: lithium iodide enriched in ^6Li (95.6%), lithium iodide enriched in ^7Li (99.9%), carbon, lead oxide, lead fluoride, aluminum, red phosphorus, scandium oxide, vanadium, and manganese. At these bombarding energies, reactions with the iodine and lead were not considered because of the high Coulomb barrier that the two elements present to the incident ^{14}N ions. The targets were made up of sufficient material so that they were thicker than the range of the incident ^{14}N beam, and were bombarded in a Faraday cup assembly so that the beam current could be integrated. The powdered target materials were pressed into $\frac{3}{4}$ -in.-diam brass molds at a pressure of 5 tons/in.². Targets prepared in this way had a smooth hard surface. Bombardment times varied with the half-life of the particular radioactive product under study.

The incident energy of the ^{14}N particles (accelerated as N^{3+}) from the 63-in. cyclotron was measured by bombarding thick carbon targets and comparing the ratio of yields per incident particle of ^{18}F and ^{24}Na with the data of Reynolds and Zucker.² This means of determining the beam energy was sensitive; at 27 MeV the relative yield of ^{18}F to ^{24}Na changes by 30% for a 4% change in the energy. Thus, a relative-yield determination of ^{18}F to ^{24}Na provides a good beam-energy measurement if the beam spread is not large. By this method, the ^{14}N incident energy was found to be 27.5 ± 0.5 MeV. The incident energy was varied by placing the appropriate nickel absorbers in front of the target in the Faraday cup. An experimental range curve for ^{14}N ions in nickel³ was used to determine the energy loss suffered by the ^{14}N beam for a given absorber. By placing the nickel absorbers directly in the Faraday cup, it became unnecessary to consider the change in charge of the ^{14}N ions as they passed through the absorbers.

The ^{14}N particles accelerated at the tandem Van de

TABLE I. Identifying radiations and branching ratios.

Product nucleus	Half-life	γ radiation (MeV)	γ -ray branching ratio (%)	Beta-ray branching ratio (%)
^{13}N	10.0 min	Annihilation radiation		100
^{14}O	125 sec	Annihilation radiation		100
^{18}F	111 min	Annihilation radiation		100
^{21}Na	23 sec	Annihilation radiation		100
^{22}Na	2.58 yr	1.28	100	
^{24}Na	15.0 h	1.37	100	
^{32}P	14.3 day	No gammas, pure β^- emitter		100
^{38}K	7.7 min	Annihilation radiation		100
^{40}Sc	3.9 h	1.16	100	
^{44}mSc	57.6 h	0.27	100	
^{52}V	3.8 min	1.43	100	
^{54}Mn	314 day	0.835	100	
^{56}Mn	2.58 h	0.845	100	

Graaff were quintuply ionized. By varying the terminal voltage from 5 to 7 MV the ^{14}N energy range from 30 to 42 MeV was covered. The ^{14}N energy was known to ± 100 keV.

After bombardment the irradiated targets were transferred to stainless steel counting cups and placed directly on a 3- \times 3-in. sodium-iodide crystal. The output of the photomultiplier tube was amplified and fed into a multichannel pulse-height analyzer. The NaI crystal was calibrated for the particular geometry by the use of several γ -ray standards. A more complete discussion of the calibration procedure has been presented earlier.⁴ The probable error in the absolute photopeak efficiencies is estimated to be 15%. The investigated reaction products could be unambiguously identified by the combination of their half-lives and γ -ray energies. The identifying half-lives, gamma radiations, and the branching ratios⁵ that were used to calculate the reaction yields are shown in Table I. Since ^{32}P emits only β^- particles, it was identified by counting the phosphorus samples, two weeks after bombardment, under shielded, calibrated thin-window Geiger counters.

III. CALCULATION OF CROSS SECTIONS

The counting rate was corrected for the NaI crystal efficiency, γ -ray branching ratio, radioactive decay during bombardment, and beam intensity to obtain the absolute yields per incident particle. For each investigated reaction the thick-target yields were determined as a function of bombarding energy. These are shown in the diagrams accompanying the discussion of the experimental results. The scatter of the data points for each reaction illustrates the relative experimental error; this error arises from uncertainties in beam intensity, counting statistics, and variation of the incident ^{14}N energy. Smooth curves were drawn through

¹ K. S. Toth and E. Newman, Phys. Rev. **130**, 536 (1963).

² H. L. Reynolds and A. Zucker, Phys. Rev. **96**, 1615 (1954).

³ H. L. Reynolds, D. W. Scott, and A. Zucker, Phys. Rev. **95**, 671 (1954).

⁴ E. Newman and K. S. Toth, Phys. Rev. **129**, 802 (1963).

⁵ *Nuclear Data Sheets*, compiled by K. Way *et al.* (Printing and Publishing Office, National Academy of Sciences—National Research Council, Washington, D. C., 1960).

the thick-target yield points and, by differentiating these curves, the cross sections were obtained as a function of the incident energy. For this determination the stopping powers were taken from the data of Northcliffe.⁶ The probable error in the absolute cross sections is estimated to be about $\pm 30\%$, taking into account uncertainties in the NaI crystal calibration, the slope of the yield curve, and in the stopping power.

IV. NUCLEON TRANSFER REACTIONS

Ten of the reactions studied proceed by the transfer of a nucleon from one interacting nucleus to the other. The yield per incident particle for these reactions is plotted versus laboratory energy in Figs. 1-3. Excitation functions obtained from these yield curves are shown in Figs. 4-6. The yield data below 20 MeV for the reaction $^{12}\text{C}(^{14}\text{N},^{13}\text{N})^{13}\text{C}$ are those of Halbert *et al.*⁷ (Fig. 1). For energies below 30 MeV the cross-section data shown in Fig. 4 for the reactions $^{16}\text{O}(^{14}\text{N},^{13}\text{N})^{17}\text{O}$ and $^{16}\text{O}(^{14}\text{N},^{15}\text{N})$ -

^{15}O are those of Halbert *et al.*⁷ and Hose and Newman,⁸ respectively. Because ZnO targets were used in the earlier investigations and PbO targets were used to obtain the present data, the reaction yields are not directly comparable. Cross sections at the same incident energies must, of course, be equal, no matter what target material is used. While the bombarding energies do not overlap, it is clear in Fig. 4 that our data agree with the earlier results.^{7,8}

The reactions $^{16}\text{O}(^{14}\text{N},^{15}\text{N})^{15}\text{O}$ and $^{12}\text{C}(^{14}\text{N},^{13}\text{N})^{13}\text{C}$ are ambiguous in that either proton or neutron transfer results in the same reaction products. Similarly, transfer of a neutron or an alpha particle leads to the same reaction products in $^{19}\text{F}(^{14}\text{N},^{15}\text{N})^{18}\text{F}$. Perkin *et al.*⁹ have previously investigated the same reaction by bombarding nitrogen with fluorine ions. Because their data disagreed with some unpublished work of Newman and

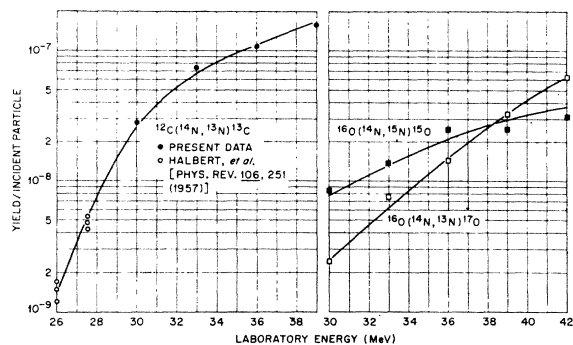


FIG. 1. Yields per incident particle for transfer reactions resulting from ^{14}N bombardment of ^{12}C and ^{16}O .

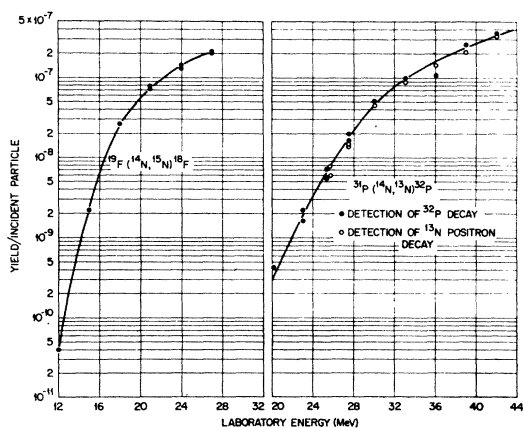


FIG. 2. Yields per incident particle for transfer reactions resulting from ^{14}N bombardment of ^{19}F and ^{31}P .

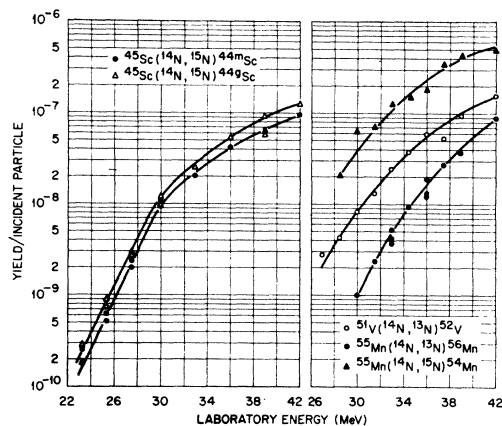


FIG. 3. Yields per incident particle for transfer reactions resulting from ^{14}N bombardment of ^{46}Sc , ^{51}V , and ^{55}Mn .

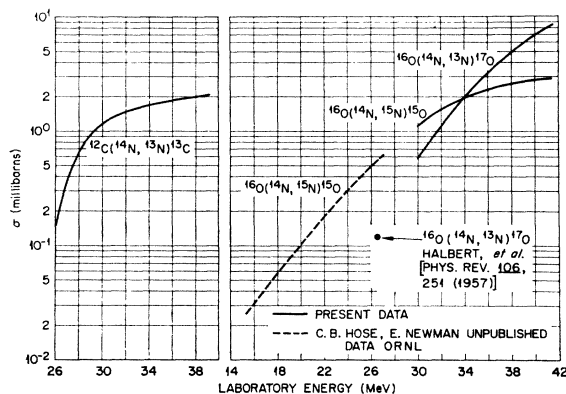


FIG. 4. Excitation functions for transfer reactions induced by ^{14}N on ^{12}C and ^{16}O .

⁶ L. C. Northcliffe, *Ann. Rev. Nucl. Sci.* **13**, 67 (1963).

⁷ M. L. Halbert, T. H. Handley, J. J. Pinajian, W. H. Webb, and A. Zucker, *Phys. Rev.* **106**, 251 (1957).

⁸ C. B. Hose and E. Newman, Oak Ridge National Laboratory (unpublished data).

⁹ J. L. Perkin, R. F. Coleman, and D. N. Herbert, *Proc. Phys. Soc. (London)* **79**, 1033 (1962).

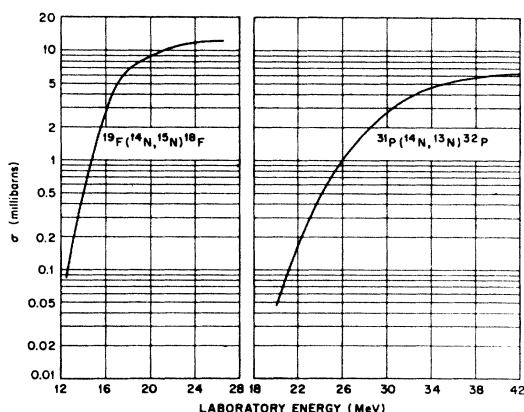


FIG. 5. Excitation functions for transfer reactions induced by ^{14}N on ^{19}F and ^{31}P .

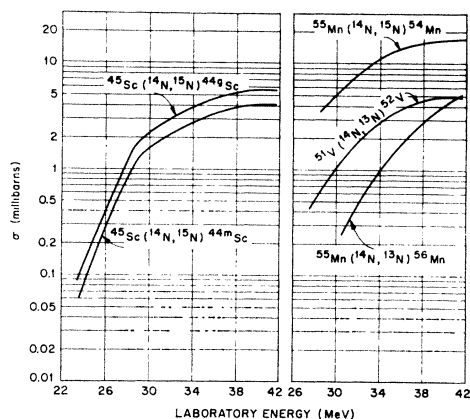


FIG. 6. Excitation functions for transfer reactions induced by ^{14}N on ^{45}Sc , ^{51}V , and ^{55}Mn .

Toth¹⁰ obtained from the ^{14}N bombardment of RbF at the same relative energy, we reinvestigated the reaction $^{19}\text{F}(^{14}\text{N}, ^{15}\text{N})^{18}\text{F}$ and found the published cross section⁹ to be low by a factor of ~ 10 .

Excitation functions have been determined for the production of ^{44m}Sc and ^{44g}Sc from the ^{14}N bombardment of ^{31}P , ^{32}S , and ^{35}Cl .¹¹ For all three reactions (which proceed through compound-nucleus formation) the ratio $^{44m}\text{Sc}/^{44g}\text{Sc}$ increases with incident energy as the compound nuclei acquire more angular momentum, and the cascade leads preferentially to the high spin metastable state. However, as shown in Fig. 6, the ratio of the cross section of the reaction $^{45}\text{Sc}(^{14}\text{N}, ^{15}\text{N})^{44m}\text{Sc}$ to that of $^{45}\text{Sc}(^{14}\text{N}, ^{15}\text{N})^{44g}\text{Sc}$ is 0.8 and remains constant with energy. This indicates that in the transfer reaction ^{45}Sc is left with essentially the same amount of angular momentum over a 20-MeV range.

The cross sections for some ^{14}N -induced reactions leading to ^{13}N were measured by observing positron

decay of ^{13}N , while others were measured by observing the decay of the nuclei which had accepted the transferred neutron. Because the excited states of ^{13}N are unstable with respect to proton emission, reactions leading to excited states of ^{13}N would not be included if the positron decay of ^{13}N were used to measure the cross section. In the reaction $^{31}\text{P}(^{14}\text{N}, ^{13}\text{N})^{32}\text{P}$, both product nuclei are radioactive. The yield for this reaction was measured by observing both the decay of ^{32}P and of ^{13}N . The two measurements gave the same result within experimental error (Fig. 2). The conclusion then is that the neutron, when transferring from ^{14}N to ^{31}P , leaves the residual ^{13}N nucleus in its ground state.

Interpretation of heavy-ion-induced nucleon transfer reactions is complicated by the complex nature of the interacting particles. However, at energies below the Coulomb barrier much of this difficulty is removed because the heavy ions do not come into contact. The tunneling theory of Breit and collaborators¹²⁻¹⁶ uses this fact to predict the variation of neutron transfer cross sections with energy, and the shape of the angular distributions of such reactions. The theory has passed through many stages of sophistication. The semiclassical formulation of the theory is used here because of its greater simplicity. The error involved in neglecting quantum corrections is less than experimental error in our cross-section measurements, e.g., for the reaction $^{14}\text{N}(^{14}\text{N}, ^{13}\text{N})^{15}\text{N}$ at bombarding energy of 14 MeV the error is $\sim 25\%$.^{12,16} It should also be noted that tunneling theory is applicable only to neutron transfer reactions satisfying rather severe limitations, e.g., $Q \approx 0$. Some reactions considered do not strictly satisfy one or more of these limitations, but past success of tunneling theory in cases which violate some limitations^{1,17} lends encouragement to its application here. For a complete discussion of the limitations of the theory see Ref. 18.

The semiclassical tunneling theory predicts the variation of total cross section σ with energy to be

$$\sigma = \frac{\Lambda^2}{8} \frac{1}{\alpha \bar{\alpha} \lambda \lambda'} \left(\frac{\alpha b_1}{1 + \alpha b_1} \right)^2 \left(\frac{\bar{\alpha} b_2}{1 + \bar{\alpha} b_2} \right)^2 \exp(X), \quad (1)$$

where

$$X = \frac{(2M)^{1/2}}{\hbar} \left[E_s^{1/2} (b_1 + b_2) \left(1 - \frac{E_B}{E} \right) + \bar{E}_s^{1/2} (\bar{b}_1 + \bar{b}_2) \left(1 - \frac{\bar{E}_B}{\bar{E}} \right) \right],$$

¹² G. Breit and M. E. Ebel, Phys. Rev. **103**, 679 (1956).

¹³ M. E. Ebel, Phys. Rev. **103**, 958 (1956).

¹⁴ G. Breit and M. E. Ebel, Phys. Rev. **104**, 1030 (1956).

¹⁵ G. Breit, in *Handbuch der Physik*, edited by S. Flügge (Springer-Verlag, Berlin, 1959), Vol. 41, Part 1.

¹⁶ G. Breit, K. W. Chun, and H. G. Wahsweiler, Phys. Rev. **133**, B403 (1964).

¹⁷ G. Breit, in *Proceedings of the Second Conference on Reactions between Complex Nuclei, Gallinburg, 1960* (John Wiley and Sons, Inc., New York, 1960), p. 1.

¹⁸ G. Breit, Phys. Rev. **135**, B1323 (1964).

¹⁰ E. Newman and K. S. Toth, Oak Ridge National Laboratory (unpublished data).

¹¹ I. R. Williams and K. S. Toth, Phys. Rev. **138**, B382 (1965).

b_1 and b_2 =radii of initial and final nuclei 1 and 2, respectively; $\Lambda = h/Mv$ =wavelength of the transferred neutron, v =relative velocity, E_s =binding energy of the neutron, $\alpha = (2ME_s/h^2)^{1/2}$, M =neutron mass, $E_B = Z_1Z_2e^2/r_0(A_1^{1/3} + A_2^{1/3})$ =Coulomb barrier, E =center-of-mass energy, and unbarred and barred quantities refer to initial and final systems respectively.

Besides the various kinematical factors, the cross-section expression [Eq. (1)] contains the product of the reduced widths in the two participating nuclei, $\lambda\lambda'$, where λ refers to the nucleus donating the neutron and λ' refers to the nucleus which has accepted the neutron. The probability of finding a neutron in a shell of unit thickness around one of these nuclei is proportional to the reciprocal of the appropriate λ .

As first suggested by Breit,¹⁷ the experimental data are replotted as $\log[\sigma(2\pi/\Lambda)^2(10^3)]$ versus X in Fig. 7 to facilitate comparison with tunneling theory. Similar plots for previously investigated nucleon transfer reactions have been presented in Refs. 1 and 17. In the region where the tunneling theory is applicable ($E < E_B$ and $\bar{E} = E + Q < \bar{E}_B$) it predicts that X should change by a factor of $\ln 10$ for an order-of-magnitude change in $\sigma(2\pi/\Lambda)^2$. The theoretical slope and the X for each reaction below which the theory is applicable are indicated in Fig. 7. In general, below the Coulomb-barrier energy the agreement of the excitation functions with the predicted slope is good except for $^{16}\text{O}(^{14}\text{N}, ^{15}\text{N})^{15}\text{O}$. Departures from the theoretical slope are possibly due to nuclear absorption at higher energies, population of excited states, and virtual Coulomb excitation for light-target nuclei far below the barrier.

Of the nucleon transfer reactions that have been investigated there are pairs of ($^{14}\text{N}, ^{13}\text{N}$) and ($^{19}\text{F}, ^{18}\text{F}$) reactions involving the same target nucleus from which one can determine values of the ratio $\lambda^{14}\text{N}/\lambda^{19}\text{F}$.¹ This is done in the following manner. The kinematical factors in formula (1) are calculable; therefore, the $\lambda\lambda'$ product for each reaction can be determined if the experimental

cross section is known. For a pair of ^{14}N - and ^{19}F -induced reactions involving a particular target, e.g., ^{10}B , two reduced width products can be calculated, $\lambda^{14}\text{N}\lambda^{11}\text{B}$ and $\lambda^{19}\text{F}\lambda^{11}\text{B}$ at an energy where the theory is expected to apply. If one then assumes that $\lambda^{11}\text{B}$ is identical for the nitrogen and fluorine reactions, then the ratio $\lambda^{14}\text{N}/\lambda^{19}\text{F}$ is determined. Each target nucleus then yields an independent value of the ratio and the similarity of the ratios gives us a consistency check of the tunneling theory. In the earlier paper¹ four ratios were obtained for the targets, ^{10}B , ^{14}N , ^{23}Na , and ^{27}Al . In the present investigation excitation functions were determined for ($^{14}\text{N}, ^{13}\text{N}$) reactions on ^{51}V and ^{55}Mn , two targets which had already been bombarded by ^{19}F ions.⁹ In addition, the $^{14}\text{N}(^{19}\text{F}, ^{18}\text{F})$ reaction was reinvestigated by bombarding a ^{19}F target with ^{14}N ions. As mentioned previously, the cross section reported by Perkin *et al.*⁹ was found to be a factor of 10 too low.

Table II gives the ratios for six reaction pairs at $X = -1.6$ which corresponds to energies where $E < E_B$ and $\bar{E} = E + Q < \bar{E}_B$ for all the listed reactions, with the exception of the value for the ^{27}Al reaction pair in

TABLE II. Reduced-width ratios.

Reaction pair	$\lambda(^{14}\text{N})/\lambda(^{19}\text{F})$
$^{10}\text{B}(^{14}\text{N}, ^{13}\text{N})^{11}\text{B}$	1.4
$^{10}\text{B}(^{19}\text{F}, ^{18}\text{F})^{11}\text{B}$	
$^{14}\text{N}(,)^{15}\text{N}$	4.6
$^{23}\text{Na}(,)^{24}\text{Na}$	1.5
$^{27}\text{Al}(,)^{28}\text{Al}$	2.0
$^{51}\text{V}(,)^{52}\text{V}$	1.1
$^{55}\text{Mn}(,)^{56}\text{Mn}$	2.6

Table II which utilizes a straight-line extrapolation of $^{27}\text{Al}(^{14}\text{N}, ^{13}\text{N})^{28}\text{Al}$ data¹⁹ obtained at energies well above $X = -1.6$. Except for the ^{14}N target the ratios agree within a factor of 2.5. The reaction $^{14}\text{N}(^{19}\text{F}, ^{18}\text{F})^{15}\text{N}$ can proceed both as a neutron transfer or as an alpha-particle transfer from ^{19}F to ^{14}N . This point is discussed further in a following section that deals with a survey of ($^{14}\text{N}, ^{18}\text{F}$) reactions induced on low- Z target nuclei. If one assumes that the two transfer mechanisms contribute about equally to the total cross section, then the $\lambda(^{14}\text{N})/\lambda(^{19}\text{F})$ ratio is reduced from 4.6 to a number which is in line with the other five ratios. The agreement between the ratios is reasonable considering that (1) the probable experimental error in the cross-section measurements is 30%, therefore the error introduced when taking a ratio of two cross sections could be as high as 60%, (2) no nuclear structure information is included in the theory, and (3) by the cancellation of the λ' in the acceptor nucleus one assumes that the same final states are being populated to the same extent for both the ^{14}N and ^{19}F reactions.

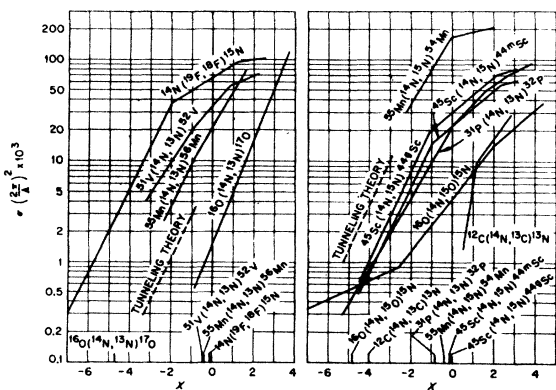


FIG. 7. Single-nucleon cross-section data plotted as $4\pi^2\sigma/\Lambda^2$ versus X ; $\Lambda = h/Mv$ =wavelength of the transferred nucleon; X is defined in Eq. (1). Tunneling theory is only applicable for each reaction at values of X less than that indicated by labeled flags.

¹⁹ V. V. Volkov, A. S. Pasiuk, and G. N. Flerov, Zh. Eksperim. i Teor. Fiz. 33, 595 (1957) [English transl.: Soviet Phys.—JETP 6, 459 (1958)].

The variation of the ratios with X is not large. As mentioned previously, $X = -1.6$ was chosen because corresponding energies are such that $E < E_B$ and $\bar{E} < \bar{E}_B$ for all targets in Table II and experimental data (except for $^{27}\text{Al}(^{14}\text{N}, ^{13}\text{N})^{28}\text{Al}$) were available at this value of X for all the reaction pairs. A value of 1.5 was used for the nuclear radius parameter r_0 to calculate the Coulomb-barrier energies. Changing the barrier height by the use of $r_0 = 1.3$ or 1.7 changes the $\lambda\lambda'$ products but again does not affect seriously the value of the ratios in Table II.

Bound-state single-particle radial wave functions may be calculated by using a Woods-Saxon potential with parameters derived from scattering experiments. These radial wave functions $R(r)$ may be compared with the quantity λ by the relation²⁰

$$-1/\lambda = r^2 R^2(r), \quad \text{where } r = 1.5A^{1/3} F.$$

Although the ground state of ^{19}F is a complicated mixture of shell-model states,²¹ we obtained a rough

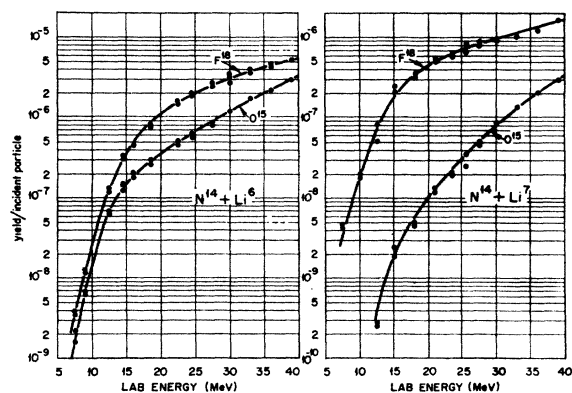


FIG. 8. Yields per incident particle for reactions resulting from ^{14}N bombardment of ^6Li and ^7Li .

estimate of $\lambda(^{14}\text{N})/\lambda(^{19}\text{F})$ in two cases by assuming $^{14}\text{N} = ^{13}\text{N} + p_{1/2}$ neutron and either (1) $^{19}\text{F} = ^{18}\text{F} + d_{5/2}$ neutron or (2) $^{19}\text{F} = ^{18}\text{F} + s_{1/2}$ neutron. For cases (1) and (2), respectively, $\lambda(^{14}\text{N})/\lambda(^{19}\text{F}) = 1.1$ and 1.4, in reasonable agreement with the ratios listed in Table II.

V. ($^{14}\text{N}, ^{18}\text{F}$) AND OTHER REACTIONS

A. ^6Li and ^7Li Targets

The yields per incident particle obtained for the lithium targets are shown in Fig. 8; the excitation functions are shown in Fig. 9.

For ^6Li the Q values are positive for the various modes of producing ^{18}F and ^{15}O . Thus, ^{18}F can be made by pn and/or d emission from the compound nucleus and also by the stripping of an alpha particle from ^6Li by the

²⁰ L. C. Becker and J. A. McIntyre, Phys. Rev. **138**, B339 (1965).

²¹ J. P. Elliot and B. H. Flowers, Proc. Roy. Soc. (London) **A229**, 536 (1955).

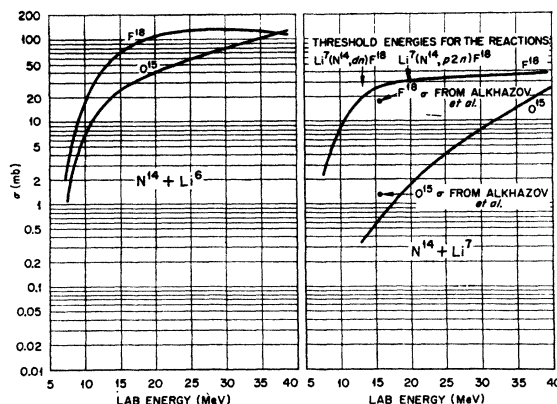


FIG. 9. Excitation functions for reactions induced by ^{14}N on ^6Li and ^7Li .

incident ^{14}N ion. Oxygen-15 can be produced by na and/or ^5He emission and also by a proton transfer from ^6Li to the ^{14}N . The resultant absence of thresholds makes it impossible to distinguish between the various modes of final nucleus production by consideration of reaction energetics alone.

For ^7Li most of the modes for producing ^{18}F and ^{15}O have negative Q values. Since the $^7\text{Li}(^{14}\text{N}, ^{18}\text{F})$ excitation function has essentially leveled off before the dn and $p2n$ threshold energies shown in Fig. 9 have been reached, the indication is that the ^{18}F is produced mainly by a mechanism with a positive Q value, i.e., triton emission from the compound nucleus $^{21}\text{Ne}^*$ or alpha-particle stripping from ^7Li by ^{14}N . Since triton production from nitrogen-induced reactions on beryllium is known to be much less than the production of either deuterons or protons,²² the excitation function shown in Fig. 9 is good evidence that the mechanism involved is alpha-particle stripping from ^7Li by the ^{14}N . The ^{15}O cross section does not level off but rather rises with increasing energy. The probable reactions for the production of ^{15}O ($\alpha 2n$ evaporation from $^{21}\text{Ne}^*$ and proton transfer from ^7Li to ^{14}N) have negative Q values. From the data it is impossible to distinguish which mechanism is involved in the reaction.

Alkhazov, Gangrskii, and Lemberg²³ irradiated a thick target of LiCl , enriched in ^7Li to 99%, with 15.6-MeV ^{14}N ions. Among other reaction products they determined the thick-target yield for ^{15}O and ^{18}F at this one bombarding energy. They assumed that below the Coulomb barrier the shapes of their excitation functions would be similar to other reactions studied by the Oak Ridge group,^{2,24-27} and in this way were able to estimate

²² C. D. Goodman and J. L. Need, Phys. Rev. **110**, 676 (1958).

²³ D. G. Alkhazov, Yu. P. Gangrskii, and I. Kh. Lemberg, Zh. Eksperim. i Teor. Fiz. **33**, 1160 (1957) [English transl.: Soviet Phys.—JETP **6**, 892 (1958)].

²⁴ H. L. Reynolds, D. W. Scott, and A. Zucker, Phys. Rev. **102**, 237 (1956).

²⁵ W. H. Webb, H. L. Reynolds, and A. Zucker, Phys. Rev. **102**, 749 (1956).

²⁶ H. L. Reynolds and A. Zucker, Phys. Rev. **100**, 226 (1955).

²⁷ H. L. Reynolds and A. Zucker, Phys. Rev. **101**, 166 (1956).

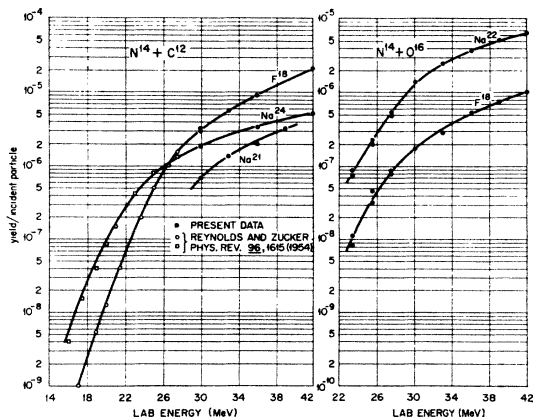


FIG. 10. Yields per incident particle for reactions resulting from ^{14}N bombardment of ^{12}C and ^{16}O .

cross sections for the investigated products at 15.6 MeV. Their $^7\text{Li}(^{14}\text{N},^{18}\text{F})$ and $^7\text{Li}(^{14}\text{N},^{15}\text{O})$ cross sections are shown in Fig. 9. Within both sets of experimental errors their cross sections are in agreement with ours.

B. ^{12}C and ^{16}O Targets

The thick-target yields for the production of ^{18}F , ^{21}Na , and ^{24}Na from carbon and ^{18}F and ^{22}Na from oxygen are shown in Fig. 10; the corresponding excitation functions are displayed in Fig. 11.

Reynolds and Zucker² obtained cross sections for the production of ^{18}F , ^{22}Na , and ^{24}Na from ^{12}C up to a ^{14}N energy of 28 MeV. Their ^{18}F and ^{24}Na yield data were combined in Fig. 10 with the results obtained in this investigation and cross sections were determined from 15 to 42 MeV. One reason for measuring $^{14}\text{N} + ^{12}\text{C}$ cross sections at available bombarding energies is that carbon is a commonly found contaminant on targets. In particular, ^{18}F , ^{22}Na , and ^{24}Na are frequently observed in ^{14}N bombardments. By knowing the excitation functions for the production of these isotopes from ^{12}C one may be able to ascertain whether the detected radio-

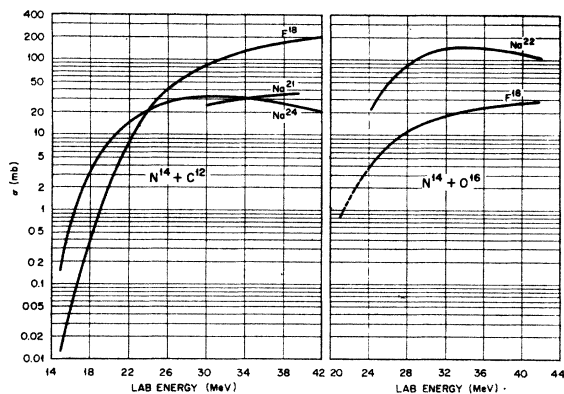


FIG. 11. Excitation functions for reactions induced by ^{14}N on ^{12}C and ^{16}O .

activity originates from the target or from the carbon contaminant. The results shown in Fig. 11 indicate that the ^{24}Na excitation function has a peak at ~ 30 MeV and then begins to drop with increasing energy; the ^{18}F curve seems to level off at ~ 42 MeV. A portion of the excitation function for the reaction $^{12}\text{C}(^{14}\text{N},\alpha\text{n})^{21}\text{Na}$ was also determined.

Previous cross-section measurements²⁴ for the production of ^{18}F from ^{16}O were extended to 42-MeV ^{14}N incident energy. In addition, the excitation function was determined for the reaction $^{16}\text{O}(^{14}\text{N},2\alpha)^{22}\text{Na}$. Since the earlier ^{18}F results²⁴ were obtained with TiO_2 targets the yield data are not included in Fig. 10. The two sets of cross-section measurements were found to agree, however, in the overlapping energy region 24–26 MeV. Therefore, in Fig. 11 the ^{18}F excitation function is shown to continue down to 21 MeV which is the lowest energy

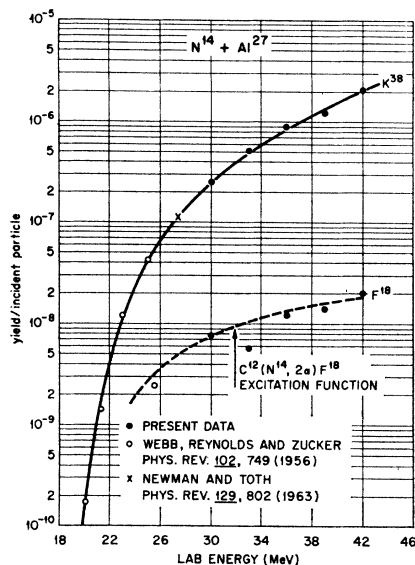


FIG. 12. Yields per incident particle for reactions resulting from ^{14}N bombardment of ^{27}Al .

at which the earlier cross-section measurements were made.

The following analysis was made of the ^{16}O results to determine whether the observed ^{18}F and ^{22}Na activities were due to carbon contamination or not. The build-up of carbon on a target results in a thin layer on the surface of the bombarded material. The yield per incident particle obtained from such a thin layer will be proportional to the cross section at the particular bombarding energy. If the radioactivity of interest is indeed produced from carbon contamination then the yield curve should match the shape of the excitation function for the production of that nuclide from ^{12}C . The ^{16}O yield curves for ^{18}F and ^{22}Na did not match with the corresponding ^{12}C excitation functions and it was concluded that the observed radioactivity was produced from ^{16}O .

TABLE III. (¹⁴N,¹⁸F) reaction data.

Target nucleus	Alpha binding energy (MeV)	σ at Coulomb barrier (mb)	Other probable direct mechanism	Target nucleus	Particles emitted	Reaction Q value (MeV)
⁶ Li	1.47	80		⁹ Be	αn	2.83
⁷ Li	2.47	23		⁶ Li	pn	0.71
⁹ Be	2.53	100		¹² C	2α	-2.88
¹⁹ F	3.99	9	neutron transfer	¹⁰ B	αpn	-3.76
¹⁰ B	4.46	3		⁷ Li	p2n	-6.54
¹⁶ O	7.15	0.7	deuteron transfer	¹⁶ O	3α	-10.1
¹² C	7.38	0.6		¹¹ B	αp2n	-15.2
¹¹ B	8.67	a		¹⁴ N	pn2α	-15.4
²⁷ Al	10.1	a		¹⁹ F	p2n3α	-30.2
¹⁴ N	11.6	a		²⁷ Al	p2n5α	-50.8

^a ¹⁸F activity due to these target materials was not observed.

Reynolds, Scott, and Zucker stated²⁴ that it was unlikely that the ¹⁸F from ¹⁶O was produced in the reaction ¹⁶O(¹⁴N,3α)¹⁸F because the Q value for the process is -10.1 MeV. This means that at 21 MeV only 1.1 MeV is available in the center-of-mass system for the emission of three alpha particles. They felt that the ¹⁸F was probably produced in the stripping-type reaction ¹⁶O(¹⁴N,¹⁸F)¹²C whose Q value was -2.73 MeV. Our measurements at higher energies rule out the possibility that the ¹⁸F is produced from carbon contamination of the target. The cross section levels off at ~20 mb at a center-of-mass energy of 17 MeV, that is, at a point where only 7 MeV is available for the emission of the three alpha particles. Again this process is unlikely to proceed. The mechanism involved is therefore probably that of deuteron transfer from the ¹⁴N and/or alpha-particle transfer from the ¹⁶O.

C. ²⁷Al Target

Measurements were made at 30-42 MeV for the production of ¹⁸F and ³⁸K from ¹⁴N bombardment of ²⁷Al. The new data are in agreement with the earlier, lower energy, yield determinations.^{4,25} In Fig. 12 we have drawn the ¹²C(¹⁴N,2α)¹⁸F excitation function normalized to the ¹⁸F thick-target yield data points. Except for one point, the ¹⁸F-from-²⁷Al data points fall close to the ¹²C(¹⁴N,¹⁸F) excitation function. By using the arguments presented in the section on ¹²C and ¹⁶O we conclude that the ¹⁸F observed at these energies from ¹⁴N incident on ²⁷Al is due mainly to carbon contamination on the aluminum target foils. Commercially obtained Al foils have been found to be contaminated with carbon.²⁸ Since only 1-2 μg/cm² of carbon contamination on the Al target foils can account for the observed yield of ¹⁸F these data cannot be considered to be evidence for the alpha-transfer reaction ²⁷Al(¹⁴N,¹⁸F)²³Na. Therefore, only the cross section for the production of ³⁸K was determined (Fig. 13).

²⁸ F. E. Durham and M. L. Halbert, Phys. Rev. **137**, B850 (1965).

VI. SURVEY OF (¹⁴N,¹⁸F) REACTIONS ON TARGETS WITH LOW ATOMIC NUMBERS

The (¹⁴N,¹⁸F) excitation functions, obtained in this investigation, were examined together with previously available results^{24,26,27} for the production of ¹⁸F from nitrogen bombardments of ⁹Be, ¹⁰B, ¹¹B, and ¹⁴N. In Table III the targets are arranged, in the extreme left-hand column, in order of increasing alpha-particle binding energy. Listed next in column 2 are the corresponding cross sections at the Coulomb barrier (calculated by using an r₀ of 1.5×10⁻¹³ cm). The supposition is that if ¹⁸F is produced by the transfer of an alpha particle from the target nucleus to the incident ¹⁴N then the cross section should exhibit some correlation with the alpha-particle binding energy of the target nucleus. If alpha transfer proceeds in a manner similar to that of nucleon transfer, then such a correlation might be expected to be reasonable, since the expression for the neutron transfer cross section [see Eq. (1)] is proportional to exp(X), where X is a term that contains the binding energy of the transferred particle. The cross section at the barrier is chosen as a convenient point of comparison because

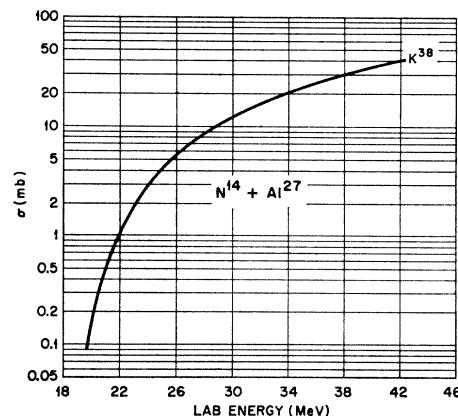


FIG. 13. Excitation function for production of ³⁸K from ¹⁴N incident on ²⁷Al.

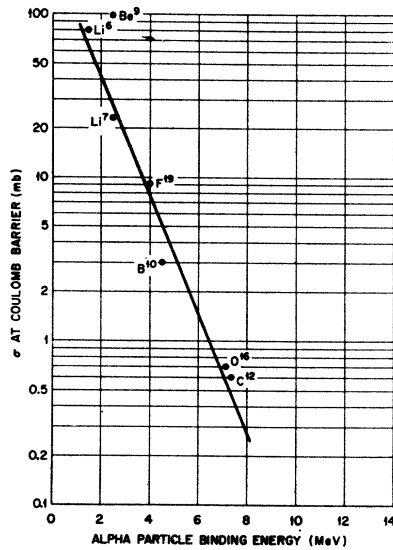


FIG. 14. Cross sections at the Coulomb barrier for ($^{14}\text{N},^{18}\text{F}$) reactions plotted as a function of the alpha-particle binding energy in the target nucleus.

transfer reactions are expected to compete best with compound-nucleus reactions at energies below and near the Coulomb barrier where the probability for fusion of the interacting nuclei is not large. The barrier cross sections are plotted in Fig. 14 as a function of alpha-particle binding energies. With the exception of ^9Be the cross sections do indeed decrease with increasing binding energy. The line drawn through the remaining points is not designed to have any theoretical significance; it is there only to show the general exponential decrease of the cross section with increasing binding energy. In column 4 it is pointed out that for ^{16}O and ^{19}F targets there are other probable transfer reactions which would result in ^{18}F , i.e., deuteron and neutron transfer from ^{14}N and ^{19}F , respectively. The targets are arranged in column 5 in order of decreasing Q value (column 7) for the most probable compound-nucleus reaction leading to ^{18}F . The ^9Be reaction has the most favorable Q value and the bulk of the measured 100 mb may be due to ($n\alpha$) evaporation from the compound nucleus; this may account for the fact that the ^9Be cross section at the Coulomb barrier is out of line with regard to the other targets.

The strong inverse dependence of the Coulomb-barrier cross sections on the target-nuclei alpha-particle binding energies suggests that at low incident energies a substantial part of the ^{18}F yield must be due to alpha-particle transfer. By considering the compound-nucleus-reaction Q value (column 7) it is clear that in the investigated energy range the $^{19}\text{F}(^{14}\text{N},^{18}\text{F})^{15}\text{N}$ cross section must be due entirely to a direct process. However, as discussed in the section on nucleon transfers, it is not possible to say how much of the cross section is due to alpha-particle transfer and how much to the transfer to a neutron from ^{19}F to ^{14}N . If it is assumed that the two mechanisms contribute equally, as was done in the nucleon transfer section (see Table II and accompanying discussion), then the ^{19}F cross section plotted in Fig. 14 would have to be reduced to ~ 4.5 mb. This value would fall somewhat below the line in Fig. 14 but would not be in disagreement with the general decrease of the cross section with increasing binding energy. We have already presented arguments as to why we believe that the ^{18}F produced from ^{14}N bombardment of ^7Li and ^{16}O is produced in direct reactions. No definite statements can be made concerning the remainder of the ($^{14}\text{N},^{18}\text{F}$) reactions listed in Table III. However, if the correlation between barrier cross sections and binding energies is meaningful, one would then assume that most of the 130-mb ^6Li cross section (Fig. 9) is due to transfer because the barrier cross section (presumably due to alpha transfer) is 80 mb. Similarly, one would conclude that the bulk of the ^9Be (see Ref. 26) and ^{12}C (see Fig. 11) cross sections, which level off at a value of ~ 200 mb, is due to the evaporation of an alpha particle and a neutron from $^{23}\text{Na}^*$ and two alpha particles from $^{26}\text{Al}^*$, respectively. Angular distribution studies will have to be made, however, to determine the mechanisms for all of the reactions discussed above.

ACKNOWLEDGMENTS

The authors wish to thank R. H. Bassel, E. C. Halbert, and M. L. Halbert for helpful comments and discussion. The direct-reaction computer program JULIE used to calculate radial wave functions was written by R. M. Drisko. The cooperation of the operating crews of the tandem Van de Graaff and the 63-in. cyclotron is gratefully acknowledged.